Pergamon

Atmospheric Environment Vol. 30, No. 3, pp. 365–378, 1996

1352-2310/96 $15.00 + 0.00

1352-2310(94)00271-1

STUDY OF THE THERMAL STRUCTURE OF A TOWN IN A NARROW VALLEY

WILHELM KUTTLER, ANDREAS-BENT BARLAG and FRANK ROßMANN
Institute of Ecology, Department of Landscape Ecology, Essen University, 45117 Essen, Germany

(*First received* 15 *October* 1992 *and in final form* 12 *August* 1994)

Abstract—This study examines the influence of urban and topoclimatic factors on the temperature field of Stolberg, Germany, a densely built up town in a valley, on the basis of stationary and mobile measurements during cloudless and nearly calm weather conditions. Qualitative and quantitative statements are made about the extent of influence by invariable parameters (percentage of sealed area, height) and by variable conditions (wind velocity, time, temperature amplitude) on thermal conditions in the investigated area. An observed influence of cold air on the temperature field near the ground required further study of wind field influences due to topographic conditions and of an analysis of intensity and frequency of valley inversions. Regarding clear and calm weather conditions, results show a significant relationship between thermal conditions and the percentage of sealed area, as well as topographical height. As a result of roughness of the built up area, the nocturnal urban excess temperature is not reduced by cold air drainage until the second half of the night. The high production of cold air causes the nocturnal component of a mountain and valley wind regime, which explains the accelerated cold air transport from above the urban canopy layer as well as the frequency of valley inversions. While ground level inversions exist in the rural area of the valley, the urban heat island effect causes an inversion at a higher level above the developed valley area.

Key word index: Stolberg, heat island effect, cold air drainage, mountain and valley wind regime, complex terrain.

1. INTRODUCTION

The positive temperature anomaly of a city in relation to its surroundings, called urban heat island, is one of the most frequently examined phenomena in the research of urban climate. Such investigations are predominantly carried out during clear and calm weather conditions and are mainly based on analyses performed in cities located in plains or wide valleys (e.g. Garstang *et al.*, 1975; Nkemdirim, 1980; Wanner and Hertig, 1984). For towns in narrow valleys only a few studies are available (e.g. Gross, 1983; Horbert *et al.*, 1991). The spatial and temporal modification of the urban heat island is not so much a result of the thermally caused air circulation like country breeze (Barlag and Kuttler, 1991), but it results from cold air dynamics due to the natural orographical structure (Goldreich, 1984; Wanner and Filliger, 1989). This study examines the problem using the town of Stolberg, located in the Vichtbach Valley in North-Rhine-Westphalia, as an example. As part of a larger research project, the target of this investigation is to analyse the influences and interactions of the town and its surroundings on the temperature field near ground level during clear and calm weather conditions. Results of further investigations concerning air exchange near the ground and air pollution are dealt with by Barlag (1993).

2. DESCRIPTION OF INVESTIGATED AREA

The investigated area is located in western Germany near the Belgian border, 20 km east of the city of Aix-la-Chapelle. It comprises an area of 10 km^2, and is characterized by a narrow notch-shaped valley in the SSE–NNW direction of approximately 500 m width, with the small river Vichtbach running through it. The relatively densely built up town centre of Stolberg (60,000 inhabitants) is located in the northern and central parts. Here, the valley narrows to 200–300 m. The town centre is surrounded in the north and south by two large industrial areas. Widespread undeveloped areas are found on the southern slopes of the valley, producing cold air during clear and calm weather conditions. The bottom of the valley has only slight inclination of 0.4° to the NNW. Generally, slopes around the valley have an inclination of 5°. The maximum difference in height between the bottom and the rim of the valley is 119 m (Fig. 1).

3. METHOD

The investigation is based on stationary and mobile measurements of air temperature, wind direction and wind velocity during the period June 1990 to April 1991. The stationary measuring network comprised eight climatological stations, which recorded the values based on hourly

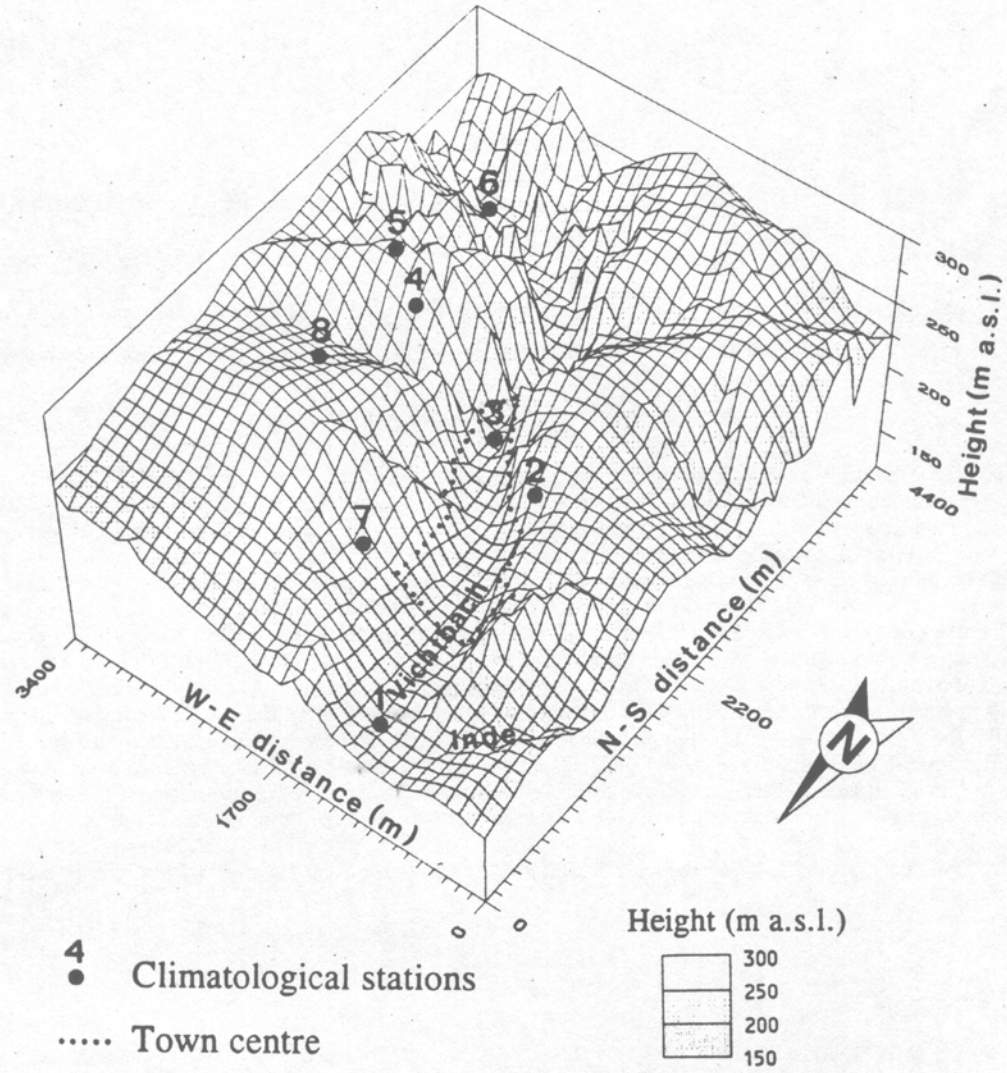

Fig. 1. Orographical structure of Stolberg area and location of climatological stations.

Table 1. Topographical characteristics of climatological stations in investigated area of Stolberg (measuring period: June 1990–April 1991)

Station	Height (m a.s.l)	Slope inclination/Exposition	Topographical characteristics
1	170	0.4°/N	North valley bottom/ industrial area
2	230	6.0°/ENE	West slope/sparsely built up area
3	185	0.4°/N	Middle valley bottom/town centre
4	250	8.0°/NNW	East slope/rural area
5	280	0.0°	Ridge/rural area
6	200	0.4°/N	South valley bottom/rural area
7	240	9.0°/WNW	North-east slope/sparsely built up area
8	265	2.7°/S	East slope/rural area

Height of thermograph: 2.0 m above ground.
Height of anemometer: 4.5 m above ground.

means. The locations of the stations are shown in Fig. 1; Table 1 contains the typical characteristics of the stations.

In addition to taking specific measurements of the air temperature at certain points, 14 mobile measurements were performed (measuring period: July 1990–July 1991) mainly during clear and calm weather conditions at night (cloud cover $< 4/8$, average wind velocity $< 2\,m\,s^{-1}$, inversion temperature conditions) to permit an analysis of air temperature over the entire area. The 65-km measuring route covered a maximum of 320 measuring points (Table 2). Time adjustments of the measured data to a reference time, necessary for the mobile measurements covering several hours, were performed on the basis of the values obtained at six climatological stations using the global trend method (Danz-

Table 2. Survey of mobile measurements in investigation area of Stolberg [temperature minimum (t_{min}), temperature maximum (t_{max}), temperature amplitude (t_{amp}), average temperature (t_{avg})]

	No.	Date	Measuring period (CET)	Chronological adjustment	Number of measuring points	Air temperature			
						t_{min} (°C)	t_{max} (°C)	t_{amp} (K)	t_{avg} (°C)
	1	11/12.07.1990	2240–0037	2330 CET	194	9.6	15.2	5.6	13.0
	2	12/13.07.1990	2240–0029	2330 CET	194	13.7	19.3	5.6	17.3
First half of the night[a]	4	20/21.07.1990	2149–0115	2330 CET	289	11.9	20.6	8.7	16.5
	6	02/03.08.1990	2138–0109	2330 CET	320	15.4	24.8	6.8	20.2
	7	24/25.08.1990	2058–0033	2230 CET	312	15.6	22.4	6.8	20.2
	10	24.10.1900	2048–2353	2200 CET	313	7.1	12.0	4.9	10.2
	12	29/30.01.1991	2201–0105	2330 CET	310	− 7.1	− 2.0	5.1	− 3.6
Windy weather[b]	13	27.02.1991	1808–2107	1930 CET	310	2.2	6.5	4.3	5.2
	3	15.07.1990	0033–0229	0130 CET	191	7.2	13.5	6.3	11.1
Second half of the night[a]	8	25.08.1990	0044–0457	0300 CET	304	13.5	20.7	7.2	17.8
	9	29.08.1990	0022–0332	0200 CET	311	13.6	19.8	6.2	16.5
	11	25.10.1990	0319–0626	0430 CET	314	6.9	11.3	4.4	9.5
Daytime measurements[a]	5	27.07.1990	1308–1639	1500 CET	302	27.3	29.5	2.2	28.5
	14	23.07.1991	1445–1827	1630 CET	307	27.0	30.4	3.4	29.0

[a]Cloudless and nearly calm weather conditions.
[b]Mesoscale wind impact.

eisen, 1983; Kuttler, 1993). Chronologically adjusted temperature differences — referred to the mean value of the area — were calculated for every measuring point and formed the basis for the statistical evaluation of the data. The statistical analysis included the following calculations:

Two-dimensional correlation:

$$r_{ab} = \frac{\sum a_i b_i - \left(\frac{1}{n}\right)\sum a_i \sum b_i}{\sqrt{\left[\sum a_i^2 - \left(\frac{1}{n}\right)(\sum a_i)^2\right]\left[\sum b_i^2 - \left(\frac{1}{n}\right)(\sum b_i)^2\right]}}, \quad (1)$$

Partial correlation:

$$r(\text{part})_{ab.c} = \frac{r_{ab} - r_{ac} - r_{bc}}{\sqrt{(1 - r_{ac}^2)(1 - r_{bc}^2)}}, \quad (2)$$

Multiple correlation:

$$r(\text{mult})_{a.bc} = \left|\sqrt{\frac{r_{ab}^2 + r_{ac}^2 - 2r_{ab}r_{ac}r_{bc}}{1 - r_{bc}^2}}\right| \quad (3)$$

with

a = chronologically adjusted temperature differences (K) referred to the mean value of the area,
b = percentage of sealed area (%),
c = topographical height (m).

Vertical profiles of air temperature, wind velocity and wind direction were obtained during suitable weather conditions by captive balloon soundings up to an altitude of 300 m above the bottom of the valley. Cold air production, i.e. heat exchange between air and earth during cloudless and nearly calm nights, was calculated with the aid of the simple approach of Wiesner (1986). This model is based on the determination of the radiation balance of low-level air taking the Ångstrøm formula for atmospheric counter radiation. For the calculation of the volume of cold air a formula which linked the radiation balance to elementary principles of heat theory was constructed. With the aid of this equation, cold air volumes can be determined, dependent on location and season.

Calculation of the volume of cold air V_0 produced during the time interval Δt has been undertaken using the approach of Wiesner (1986):

$$V_0 = \frac{A_B a_{st}(\alpha - \beta \cdot 10^{-\chi e_0})(\overline{\vartheta_L - \vartheta_B})\Delta t F}{c_p \Delta\vartheta} \quad (4)$$

with

(1) $(\overline{\vartheta_L - \vartheta_B}) = [\alpha/(\beta + 1)(\beta + 2)]H^{\beta+1} + \vartheta_B$

and it is the mean temperature difference of cold air volume and air temperature at surface level. Here H is the height of the inversion and $\alpha = 0.820$, $\beta = 0.250$, $\chi = 0.126$ are the constants of the Ångstrøm term.

(2) c_p is mean specific heat of cold air with p = const. between ϑ_L and ϑ_B which is spatial mean temperature of cold air volume neglecting outgoing radiation.
(3) $\Delta\vartheta$ is total temperature drop at max. H (m).
(4) A_B is ratio of absorbed to reflected energy.
(5) a_{st} is radiation coefficient.
(6) F is area of cold air production (m²).
(7) e_0 is nocturnal vapour pressure (mmHg).

4. RESULTS

To determine qualitative and quantitative influences of anthropogenic and natural factors on the heat island intensity of Stolberg, air temperature differences, referred to the mean value of the area, were compared with the various influencing parameters by correlation and regression analyses. Invariable parameters were the percentage of sealed area, i.e. the area of streets, places, buildings in percent of the reference area of 200 m², calculated for each measuring point and topographical height. Wind velocity, time factor and temperature amplitude were chosen as variable marginal conditions (Section 4.2).

In the course of the investigation, special emphasis was attached to the behaviour of cold air in the valley,

since it was found that the nocturnal cold air drainage during clear and calm weather conditions is a determining element for the intensity of the heat island effect. Because of the time-dependent production and transport of cold air, a distinction was made in the assessment of the first half (1800 to 2400 CET) and second half of the night (0000 to 0600 CET).

4.1. *Influence of invariable parameters*

Based on the two-dimensional, partial and multiple correlation analyses (Table 3), investigation of the invariable parameters percentage of sealed area (*b*) and height (*c*) on the temperature field near the ground (*a*) showed a significant correlation between the temperature distribution and the rate of sealed area. The extent of the correlation (r_{ab}) can be evaluated as moderate to distinct. The analyses have shown that the positive correlation between temperature distribution and percentage of sealed area is more distinct in the first half of the night than in the second half. Even during the day (mobile measurements No. 5 and 14), as well as during mobile measurement during nighttime at windy weather (mobile measurement No. 13), the positive correlation remains. A less distinct correlation is also found between temperature distribution and height of the area (r_{ac}). Positive correlation coefficients indicate a temperature increase in line with increasing altitude, while negative correlation coefficients indicate a temperature decrease with increasing altitude. In contrast to the percentage of sealed area, the correlation to height is more distinct in the second half of the night. Results of the three-dimensional correlation analysis [$r(\text{mult})_{a.bc}$] show that the distribution of air temperature is more easily explicable by the bilateral influence of sealing and height. Regarding calm and clear weather conditions, up to 52% of measured air temperatures are attributable to the influence of these two factors. A highly significant correlation of the combined influence of the fraction of sealed area and height on the temperature field was shown by three-dimensional linear regressional and multiple correlation analysis to quantify the degree of influence.

During cloudless conditions at night, the influence of the percentage of sealed area on the temperature field in the investigated area shows an increase in air temperature by an average of 0.35 K per 10% sealed area (Table 4). In addition to this anthropogenic excess temperature caused by the sealed area, natural excess heating takes place on the slopes and rounded hilltops (thermal belt) during cloudless weather conditions with air temperatures that may be higher than those of the urban area. This is verified by the positive regression coefficients (*C*) (Table 4), which show temperature increases from 0.5 to 4 K for 100 m. To assess

Table 3. Results of two-dimensional (r) and multiple correlation analysis [r(mult)] to determine relationship between temperature (*a*), percentage of sealed area (*b*), and height of area (*c*) in Stolberg. Data basis: 14 mobile measurements between July 1990 and July 1991. No. = Number of mobile measurements; n = number of measuring points

	No./n		r_{ab}	$\hat{t}_{ab}$*	r_{ac}	$\hat{t}_{ac}$*	$r(\text{mult})_{a.bc}$	$\hat{F}$**
	1	$n = 194$	0.59	10.1	− 0.18	− 2.5	0.61	113.78
	2	$n = 194$	0.68	12.9	− 0.24	− 3.4	0.69	174.48
First half of	4	$n = 289$	0.52	10.3	0.05	0.8	0.62	179.21
the night[a]	6	$n = 320$	0.35	6.7	0.41	8.0	0.72	341.22
	7	$n = 312$	0.48	9.6	0.05	0.9	0.56	141.63
	10	$n = 313$	0.27	5.0	0.29	5.4	0.54	124.43
	12	$n = 310$	0.27	4.9	0.22	4.0	0.46	82.66
Windy weather[b]	13	$n = 310$	0.58	12.5	− 0.74	− 19.3	0.79	511.37
	3	$n = 191$	0.19	2.7	0.41	6.2	0.61	112.00
Second half of	8	$n = 304$	0.24	4.3	0.32	5.9	0.54	124.31
the night[a]	9	$n = 311$	0.40	7.7	0.17	3.0	0.55	134.01
	11	$n = 314$	0.14	2.5	0.56	11.9	0.71	317.16
Daytime	5	$n = 302$	0.43	8.2	− 0.45	8.7	0.51	105.46
measurements[a]	14	$n = 307$	0.47	9.3	− 0.57	− 12.1	0.62	190.45

* Significance limits of the t-test:

$$t\,(\Phi = 150;\ \alpha = 0.01_{\text{bilateral}}) = 2.61,$$
$$t\,(\Phi = 200;\ \alpha = 0.01_{\text{bilateral}}) = 2.60,$$
$$t\,(\Phi = 300;\ \alpha = 0.01_{\text{bilateral}}) = 2.59,$$

** Significance limits of the F-test:

$$F\,(\Phi_1 = 1;\ \Phi_2 = 100;\ \alpha = 0.01_{\text{bilateral}}) = 6.90,$$
$$F\,(\Phi_1 = 1;\ \Phi_2 = 200;\ \alpha = 0.01_{\text{bilateral}}) = 6.76.$$

[a] Cloudless and nearly calm weather conditions.
[b] Mesoscale wind impact.

Table 4. Three-dimensional regression models ($a = A + Bb + Cc$) to determine temperature differences to mean value of area (a) as a function of percentage of sealed area (b) and height of area (c) in Stolberg. Data basis: 14 mobile measurements between July 1990 and July 1991. No. = Number of mobile measurements, n = number of measuring points

	No./n		Regression coefficients A	B	C
First half of the night[a]	1	$n = 194$	− 2.66	0.03	0.006
	2	$n = 194$	− 2.71	0.04	0.005
	4	$n = 289$	− 5.73	0.05	0.02
	6	$n = 320$	− 12.27	0.06	0.04
	7	$n = 312$	− 5.01	0.04	0.015
	10	$n = 313$	− 4.97	0.03	0.02
	12	$n = 310$	− 3.89	0.02	0.01
Windy weather[b]	13	$n = 310$	2.33	0.0096	− 0.01
Second half of the night[a]	3	$n = 191$	− 7.09	0.03	0.03
	8	$n = 304$	− 6.47	0.03	0.02
	9	$n = 311$	− 4.18	0.03	0.01
	11	$n = 314$	− 6.00	0.02	0.02
Daytime measurements[a]	5	$n = 302$	0.69	0.005	− 0.004
	14	$n = 307$	1.76	0.009	− 0.009

[a]Cloudless and nearly calm weather conditions.
[b]Mesoscale wind impact.

Table 5. Two-dimensional correlation coefficients and linear regression analysis to determine influence of percentage of sealed area (b) on temperature differences to mean of area (a), referring to bottom of Vichtbach Valley. Data basis: 14 mobile measurements between July 1990 and July 1991. Regression equation: $a = A + Bb$, $b_a > 0$ (%) = percentage of sealed area, when positive temperature anomalies can be expected in the Vichtbach Valley, No. = number of mobile measurements, n = number of measuring points, Si = significance limits of the correlation coefficients (Φ_{n-2}; $\alpha = 0.01_{\text{bilateral}}$)

	No./n		Correlation r_{ab}	Si ($\alpha = 0.01$)	Regression A	B	$b_{a>0}$ (%)
First half of the night[a]	1	$n = 69$	0.81	0.32	− 2.17	0.04	> 54.3
	2	$n = 70$	0.88	0.32	− 2.50	0.05	> 50.0
	4	$n = 79$	0.88	0.30	− 3.08	0.05	> 73.6
	6	$n = 92$	0.86	0.27	− 4.66	0.06	> 77.7
	7	$n = 86$	0.83	0.28	− 4.05	0.06	> 67.5
	10	$n = 86$	0.80	0.28	− 2.88	0.03	> 96.0
	12	$n = 84$	0.79	0.28	− 2.92	0.04	> 73.0
Windy weather[b]	13	$n = 85$	0.71	0.28	− 0.10	0.02	> 5.0
Second half of the night[a]	3	$n = 68$	0.85	0.32	− 3.32	0.05	> 66.4
	8	$n = 84$	0.86	0.28	− 3.94	0.05	> 78.8
	9	$n = 84$	0.85	0.28	− 2.44	0.04	> 61.0
	11	$n = 86$	0.62	0.28	− 1.96	0.02	> 98.0
Daytime measurements[a]	5	$n = 84$	0.44	0.28	− 0.26	0.008	> 32.5
	14	$n = 81$	0.28	0.28	− 0.20	0.007	> 28.6

[a]Cloudless and nearly calm weather conditions.
[b]Mesoscale wind impact.

the influence of sealed areas on the temperature field near the ground, correlation and regression analyses were based exclusively on data measured in the very slightly inclined valley with its heterogeneous utilization. If r^2 is calculated on the basis of single correlation coefficients (Table 5), it follows that excess temperatures prevailing in the valley during clear and calm weather conditions depend up to 77% upon the influence of the fraction of sealed area. With the help of the regression coefficients in Table 5, it is likewise possible to determine the percentage of sealed area required to cause a positive temperature anomaly compared to the mean value of the sealed area in the valley ($b_{a>0}$). Considerable differences exist between the series of data obtained by mobile measurements. During the night the percentage of 54 to 98% of

sealed area is necessary to cause excess heating. The extraordinary difference between these values prove that the excess temperature of a town in a valley could be influenced considerably by nocturnal cold air drainage.

For the interpretation of these results, constant influences must be regarded as parameters, which are the fundamental prerequisites for differences in urban and rural climate within the area examined. The differences between the correlation coefficients, however, clearly show that the extent of correlation between the temperature and the parameters discussed depends on additional factors found in the field of the variable factors of influence.

4.2. *Influence of variable parameters*

Variable parameters, expected to have an influence on the correlation between temperature and sealing, as well as between temperature and height in the investigated area, are as follows:

- *Mean wind velocity of area* (x). Calculation of the mean velocity in the area during periods with mobile measurements was performed on the data basis of stations No. 1–8.
- *Time factor* (z). The time used for statistical purposes was the adjusted time (CET) of the mobile measurements, with minutes expressed in decimals.
- *Maximum temperature amplitude in area during the period of mobile measurements* (y), *as well as mean temperature amplitude of day measurements were taken* (w), *calculated on the basis of data obtained at climatological stations.* Temperature amplitudes determined from the mobile measurements can indirectly be regarded as a measure of long wave radiation conditions. Good conditions for long wave radiation from the ground are linked to considerable temporal contrasts in temperature. High temperature amplitudes are linked with a high rate of cold air generation by radiative loss and corresponding surface-based radiative temperature inversions.

Table 6 shows a survey of the influence of the above-mentioned variable parameters on correlations between temperature (a), sealing (b), and height (c). Values shown are correlation coefficients between correlations [r_{ab}, r_{ac}, $r(\text{part})_{ab.c}$, $r(\text{part})_{ac.b}$] and the variable factors of influence.

The influence of variable parameters on the correlation between temperature and sealing (r_{ab}) can only be proved in a limited extent in the investigated area, as the correlation coefficients are considerably below the significance level of $\alpha = 0.01$ at given number of measurements at $|r| \leqslant 0.66$. Only the correlation between the partial correlation approach [$r(\text{part})_{ab.c}$] and the temperature amplitude for mobile measurements (y) indicates a significant result, i.e. $r = 0.74$. The correlations between temperature (a) and height (c) are, on the other hand, determined by both wind velocity (x) and time (z), thus ensuring a significance level of $\alpha = 0.01$. Figure 2 shows that temperature inversions mainly occur in the second half of the night at low wind velocities. At wind velocities above 2.5 m s^{-1} it is no longer possible to have inversions even in the second half of the night. During daytime, high wind velocities are linked to decreasing temperature with height. The influence of the fraction of sealed area on the thermal structure is characteristic of the first half of the night, and is verified by a steep increase of the regression area in line with increasing sealing. On the bottom of the valley (160–200 m a.s.l.), negative temperature anomalies of up to -1.7 K were calculated for undeveloped areas, compared to the average temperature of 13°C in the area (Fig. 3). Excess temperatures of up to 3 K were determined for totally sealed areas. There is only a slight temperature increase with increasing altitude. It is therefore reasonable to assume a negative temperature anomaly of about -1 K for unsealed areas at an altitude of 280 m a.s.l. At a temperature increase of 0.3 K per 10% sealed area—with a comparably high percentage of sealed area of 80% in the town centre—positive

Table 6. Influence of variable parameters on correlation between temperature (a) and percentage of sealed areas (b) as well as between temperature (a) and height of area (c); shown as results of two-dimensional correlations (r) and partial correlations [r (part)]. Data basis: 14 mobile measurements between July 1990 and July 1991. Si = Significance limits of correlation coefficients (Φ_{n-2}; $\alpha = 0.01_{\text{bilateral}}$): $|r| = 0.66$

Variable parameters	Influence of variable parameters on correlation			
Mean wind velocity (m s^{-1}) in area (x)	$r = 0.33$	$r = -0.64$	$r = -0.83$	$r = -0.88$
Time (CET) (z)	$r = -0.38$	$r = 0.64$	$r = 0.83$	$r = 0.85$
Maximum temperature amplitude (K) during mobile measurements (y)	$r = -0.01$	$r = 0.74$	$r = 0.54$	$r = 0.62$
Mean of stationary temperature amplitude (K) during day (w)	$r = -0.07$	$r = 0.55$	$r = 0.52$	$r = 0.60$
	r_{ab}	$r(\text{part})_{ab.c}$	r_{ac}	$r(\text{part})_{ac.b}$
	Correlation between temperature (a), percentage of sealed areas (b), and height (c)			

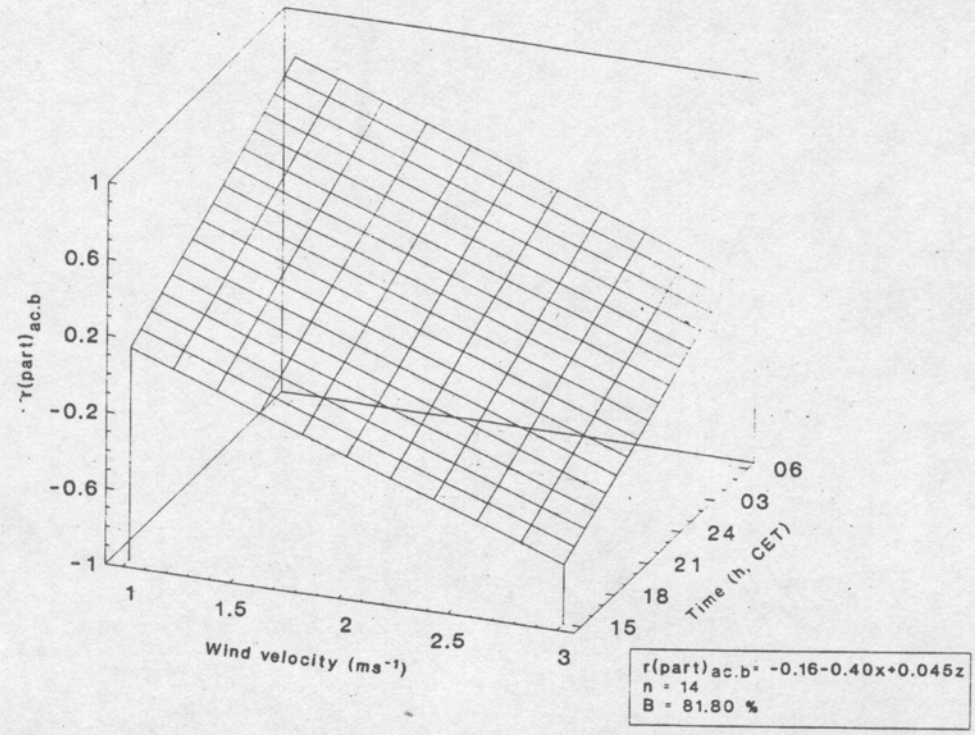

Fig. 2. Correlation between temperature (*a*) and topographical height of area (*c*), excluding percentage of sealed area (*b*) [r (part)$_{ac.\,b}$], as function of wind velocity (*x*) and time (*z*), based on data obtained from 14 mobile measurements during July 1990 and July 1991.

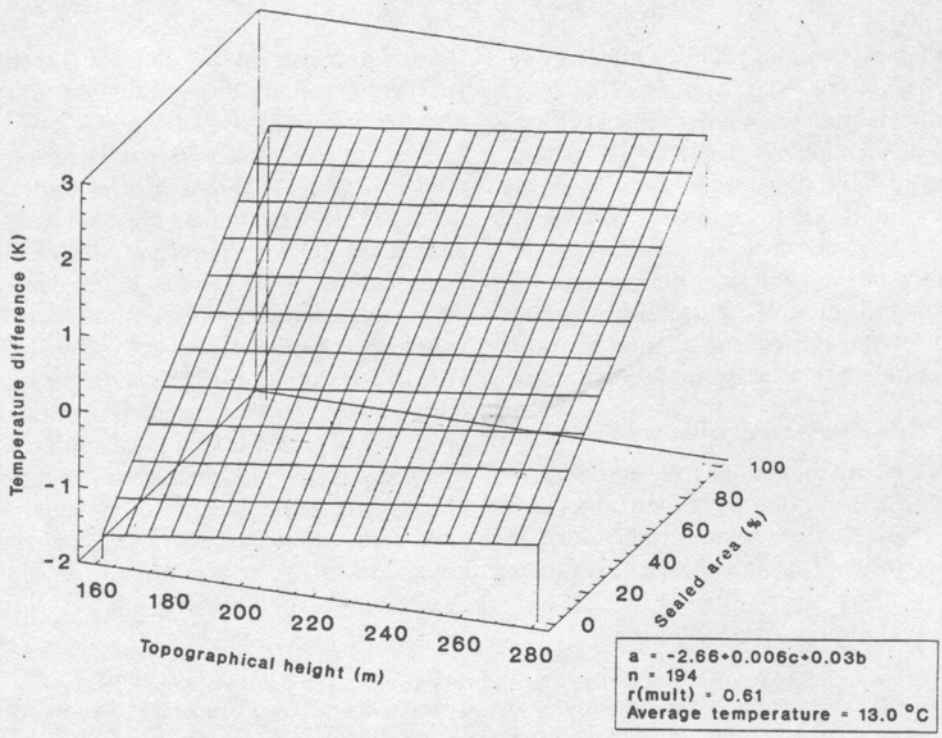

Fig. 3. Dependence of temperature differences (*a*) on topographical height of area (*c*) and percentage of sealed area (*b*) during cloudless and nearly calm weather conditions in first half of the night between 1800 and 2400 CET (11/12.07.1990) in Stolberg.

temperature anomalies between 0.7 and 0.9 K occurred in the Vichtbach Valley. Figure 4 shows that the entire valley is characterized by negative temperature anomalies during the second half of the night, even in highly sealed areas. In addition, a considerably higher increase in temperature with height is shown for the second half of the night, compared to the first half. The thermal influence is much more

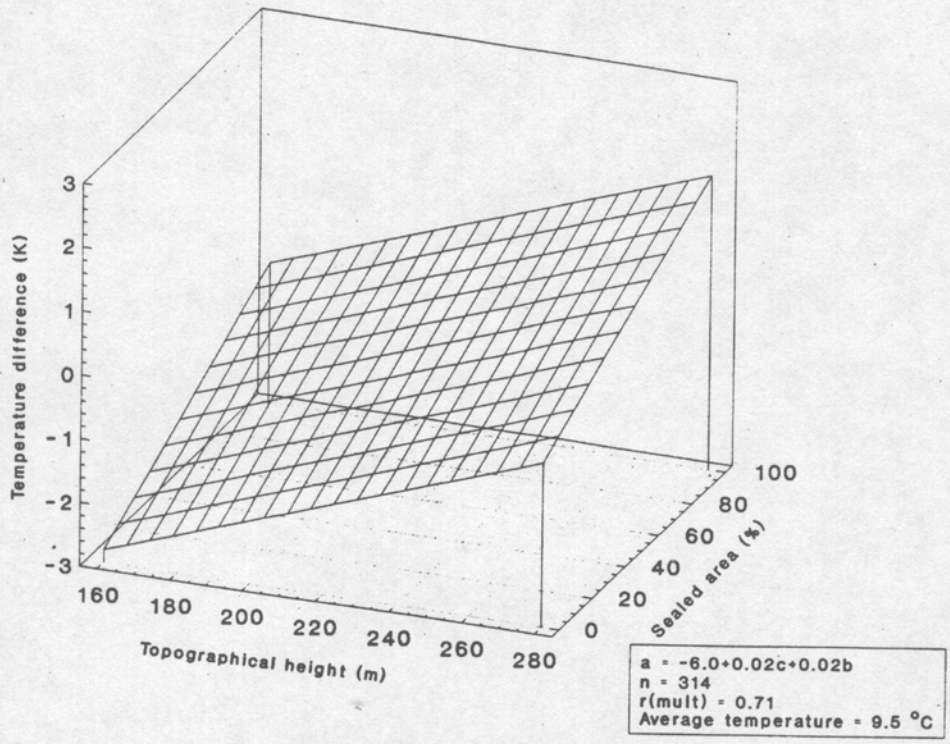

Fig. 4. Dependence of temperature differences (*a*) on topographical height of area (*c*) and percentage of sealed area (*b*) during cloudless and nearly calm weather conditions in second half of the night between 0000 and 0600 CET (25.10.1990) in Stolberg.

evident in the thermal belt and rounded hilltops during the second half of the night.

This result indicates that in an orographically formed region like the Vichtbach Valley cold air generation and drainage have a modifying effect on the temperature conditions of a town located in a valley, in addition to the influence of sealed area and height.

The importance of the cold air drainage near the ground for the modification of the urban heat island was the reason for the subsequent quantification of the cold air potential and the analysis of its dynamics.

4.3. *Analysis of cold air potential and dynamics*

In the area under investigation, five regions produce cold air, with an overall area comprising 4 km^2 (40% of entire area). As these regions are located in the southern part, the cold air flows in the direction of the town centre. In the following section, cold air generation will be dealt with first, followed by an analysis of cold air transport.

Cold air potential. On the basis of the applied model of Wiesner (1986), a total cold air volume of 875×10^6 m^3 per cloudless night was calculated as the annual average for all areas producing cold air in the investigated region (Table 7). In purely arithmetic terms, this volume is sufficient to renew the entire air volume of the valley (145×10^6 m^3) six times per night. Due to the varying night periods, the seasonal distribution is as follows: in spring the volume of cold air produced per night is virtually identical to the annual average value, while summer shows the smallest rate of cold air production. The long winter nights generate a considerably larger volume of cold air, amounting to 1367×10^6 m^3 according to the applied model.

Table 7. Size of cold air producing areas and volume of cold air during one cloudless and nearly calm night averaged for one year and by season in Stolberg. Calculation based on the approach of Wiesner (1986)

Area	(m^2)	Spring (10^6 m^3)	Summer (10^6 m^3)	Autumn (10^6 m^3)	Winter (10^6 m^3)	Year (10^6 m^3)
1	124,300	27.7	16.9	22.2	42.4	27.1
2	463,080	101.4	59.3	81.4	155.2	99.3
3	2,409,250	522.7	302.6	418.5	800.0	511.9
4	1,031,290	229.3	134.1	343.3	351.1	224.6
5	56,080	12.5	7.3	10.0	19.1	12.2
$\sum$	4,084,000	893.6	520.2	875.4	1367.8	875.1

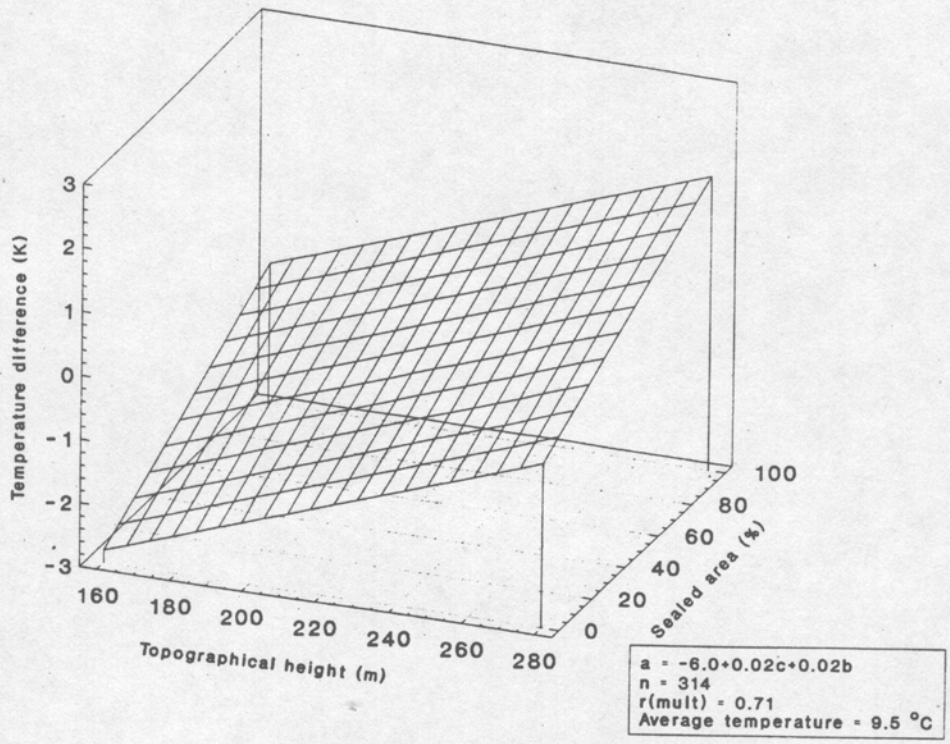

Fig. 4. Dependence of temperature differences (*a*) on topographical height of area (*c*) and percentage of sealed area (*b*) during cloudless and nearly calm weather conditions in second half of the night between 0000 and 0600 CET (25.10.1990) in Stolberg.

evident in the thermal belt and rounded hilltops during the second half of the night.

This result indicates that in an orographically formed region like the Vichtbach Valley cold air generation and drainage have a modifying effect on the temperature conditions of a town located in a valley, in addition to the influence of sealed area and height.

The importance of the cold air drainage near the ground for the modification of the urban heat island was the reason for the subsequent quantification of the cold air potential and the analysis of its dynamics.

4.3. *Analysis of cold air potential and dynamics*

In the area under investigation, five regions produce cold air, with an overall area comprising 4 km^2 (40% of entire area). As these regions are located in the southern part, the cold air flows in the direction of the town centre. In the following section, cold air generation will be dealt with first, followed by an analysis of cold air transport.

Cold air potential. On the basis of the applied model of Wiesner (1986), a total cold air volume of 875×10^6 m^3 per cloudless night was calculated as the annual average for all areas producing cold air in the investigated region (Table 7). In purely arithmetic terms, this volume is sufficient to renew the entire air volume of the valley (145×10^6 m^3) six times per night. Due to the varying night periods, the seasonal distribution is as follows: in spring the volume of cold air produced per night is virtually identical to the annual average value, while summer shows the smallest rate of cold air production. The long winter nights generate a considerably larger volume of cold air, amounting to 1367×10^6 m^3 according to the applied model.

Table 7. Size of cold air producing areas and volume of cold air during one cloudless and nearly calm night averaged for one year and by season in Stolberg. Calculation based on the approach of Wiesner (1986)

Area	(m^2)	Spring (10^6 m^3)	Summer (10^6 m^3)	Autumn (10^6 m^3)	Winter (10^6 m^3)	Year (10^6 m^3)
1	124,300	27.7	16.9	22.2	42.4	27.1
2	463,080	101.4	59.3	81.4	155.2	99.3
3	2,409,250	522.7	302.6	418.5	800.0	511.9
4	1,031,290	229.3	134.1	343.3	351.1	224.6
5	56,080	12.5	7.3	10.0	19.1	12.2
$\sum$	4,084,000	893.6	520.2	875.4	1367.8	875.1

This large volume of cold air, however, does not prevent the occurrence of excess heating in the central and northern Vichtbach Valley during the first half of the night. Consequently, it must be assumed that the cold air drainage within the urban canopy layer (UCL) can only penetrate with a delay into the densely built up regions of the valley because of man made and orographic barriers. This would explain the thermal structure, which is more or less independent of the cold air generation during the first half of the night. As, apart from cold air formation, cold air transport has a considerable effect on the thermal structure of the town, a detailed analysis was performed to investigate this phenomenon.

Cold air dynamics. Examination of cold air dynamics near the ground, based on mobile measurements, shows different degrees of penetration of cold air into the urban area as a function of time. As Fig. 5 shows, cold air masses advancing from the southern part of the investigated area before 2330 CET reach at least the fringe of the heavily built up area. Cold air flows around or over the southern industrial area in the first half of the night. The entire southern region of the valley proves to be an area where cold air accumulates and which shows high negative temperature anomalies.

The low penetration of the cold air between 2230 and 2330 CET within the valley proves the above thesis that the cold air cannot flow away to the north unobstructed during the first half of the night. At the narrowest point of the Vichtbach Valley, the orographic constriction of the valley, in combination with the built up area and the roughness, form an obstacle for any cold air influx near the ground. This causes

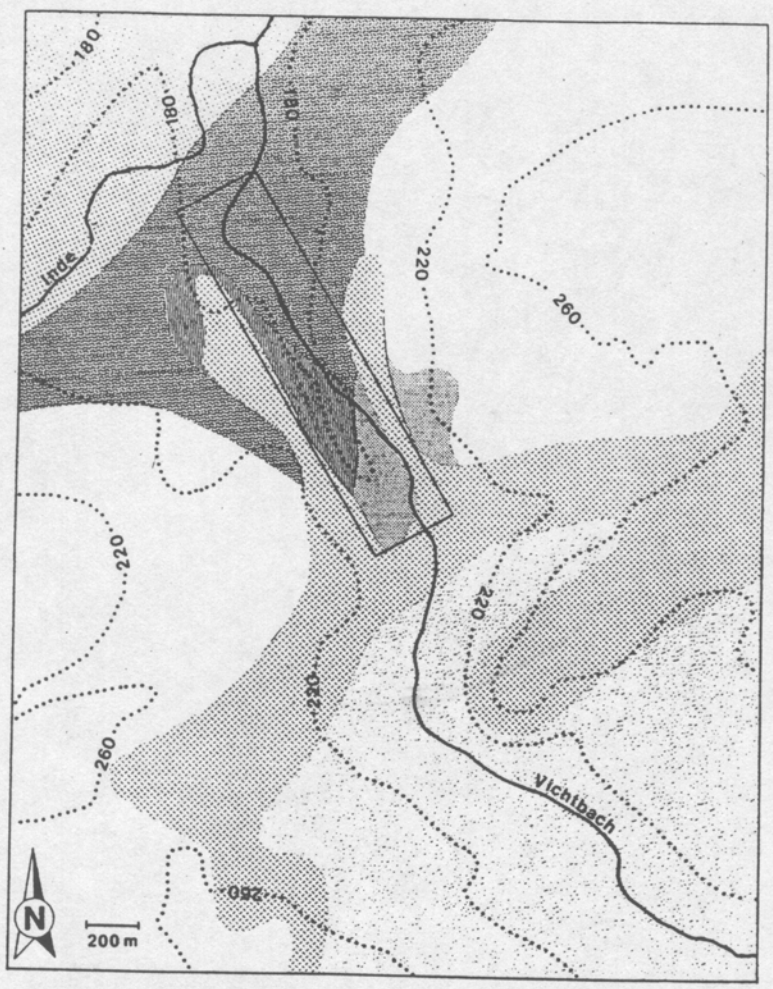

Minimum cold air penetration between 2230 and 2330 CET
Maximum cold air penetration between 2230 and 2330 CET
Maximum cold air penetration until 0130 CET
Maximum cold air penetration until 0200 CET
Maximum cold air penetration until 0430 CET
Town centre
····· Topographical height (m)

Fig. 5. Dynamics of cold air penetration during cloudless and nearly calm weather conditions in measuring period from July 1990 to July 1991.

a considerable stagnation of cold air in Stolberg, in conjunction with the slight inclination of the valley bottom. Due to this, there are high urban–rural temperature differences of up to 6 K during the first half of the night. As the cold air regions are on eastern and western sides of the town, it can be assumed that the cold air flows around or over the town centre. Whereas cold air can only advance slowly into the valley until 0200 CET because of the built up area, the entire Vichtbach Valley may be filled with cold air by 0430 CET. This is illustrated in Fig. 6 which shows the spatial distribution of temperature differences between two consecutive mobile measurements during the first and during the second half of the night. The highest temperature difference ($\Delta t = 4$ K) mainly took place in the densely built up areas at the bottom of the valley. The slopes and rounded hilltops are characterized by a considerably lower cooling rate between the first and second half of the night.

Wind field examinations during 41 cloudless days with low winds showed that cold air drainage at ground level reached a mean velocity of 0.9 m s^{-1}, with twice the velocity in the urban boundary layer (UBL) located above (Table 8).

In the UBL of the valley, it can be reasonably assumed that higher wind velocities will prevail, so that the real cold air drainage happens above the UCL. This spatial distribution clearly also occurs during the day; however, wind velocities are higher. This diurnal variation of wind velocities is due to a mountain and valley wind system separated from the geostrophic wind regime, as illustrated by the wind roses in Fig. 7. A canalization effect, due to the course of the valley, can be observed. This also results

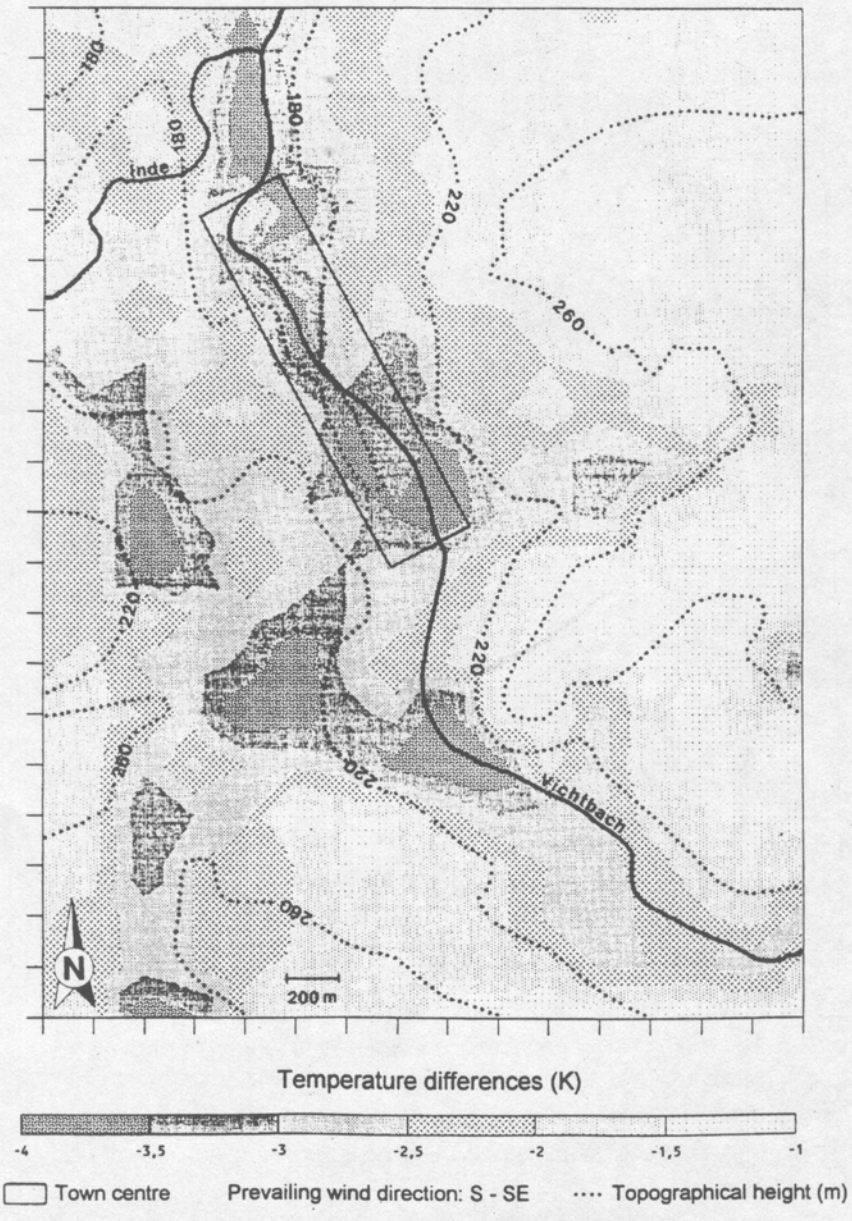

Fig. 6. Temperature differences (K) between 2230 and 0300 CET (24/25.08.1990) during cloudless and nearly calm weather conditions in Stolberg.

Table 8. Mean values of wind velocity ($m\ s^{-1}$) during nocturnal mountain and daytime valley wind regimes. Day = 0700–1800 CET. Data basis: 41 cloudless days in the period of investigation between June 1990 and April 1991

Stations	Day	Night
Mean of area		
Stations 1–7	2.1	1.5
Valley bottom		
Stations 1, 3, and 6	1.7	0.9
Slope area		
Stations 2, 7, and 4	2.3	1.8
Ridge		
Station 5	3.0	1.9

in different frequencies of occurrence of this circulation system at various locations in the valley.

The cold air in the Vichtbach Valley often causes isothermal and inversion temperature layers with dependence of the percentage of sealed area. The southern valley is characterized by a rate of 56% of inversion conditions, between the bottom of the valley and the upper slope zones, the region with most inversions (Table 9). In comparison, the vertical temperature profile between the town centre and the rounded hilltops (Stations 3 and 4) only reflects 25% of such hours, which clearly shows the influence of heat islands on the occurrence of inversions. Another point investigated was the height to which this urban heat island effect extends. Analysis of the vertical distribution of air layers from the bottom of the valley to the lower slopes in the southern valley (Stations 6 and 2), nearly the same percentage of hours (52%) was determined, while a considerably lower rate of 25 to 15% was found in the central part of the valley. This shows that the thermal effects of the development in the town centre often extend to the height of Station 2 (35 m above the valley bottom), as from this altitude the inversion is lifted off above the town centre (Fig. 8). During the time of a steady ground level inversion, which lasted for eight days in the southern valley (Stations 6 and 4), inversion layers were seldom observed between the town centre and rounded hill-

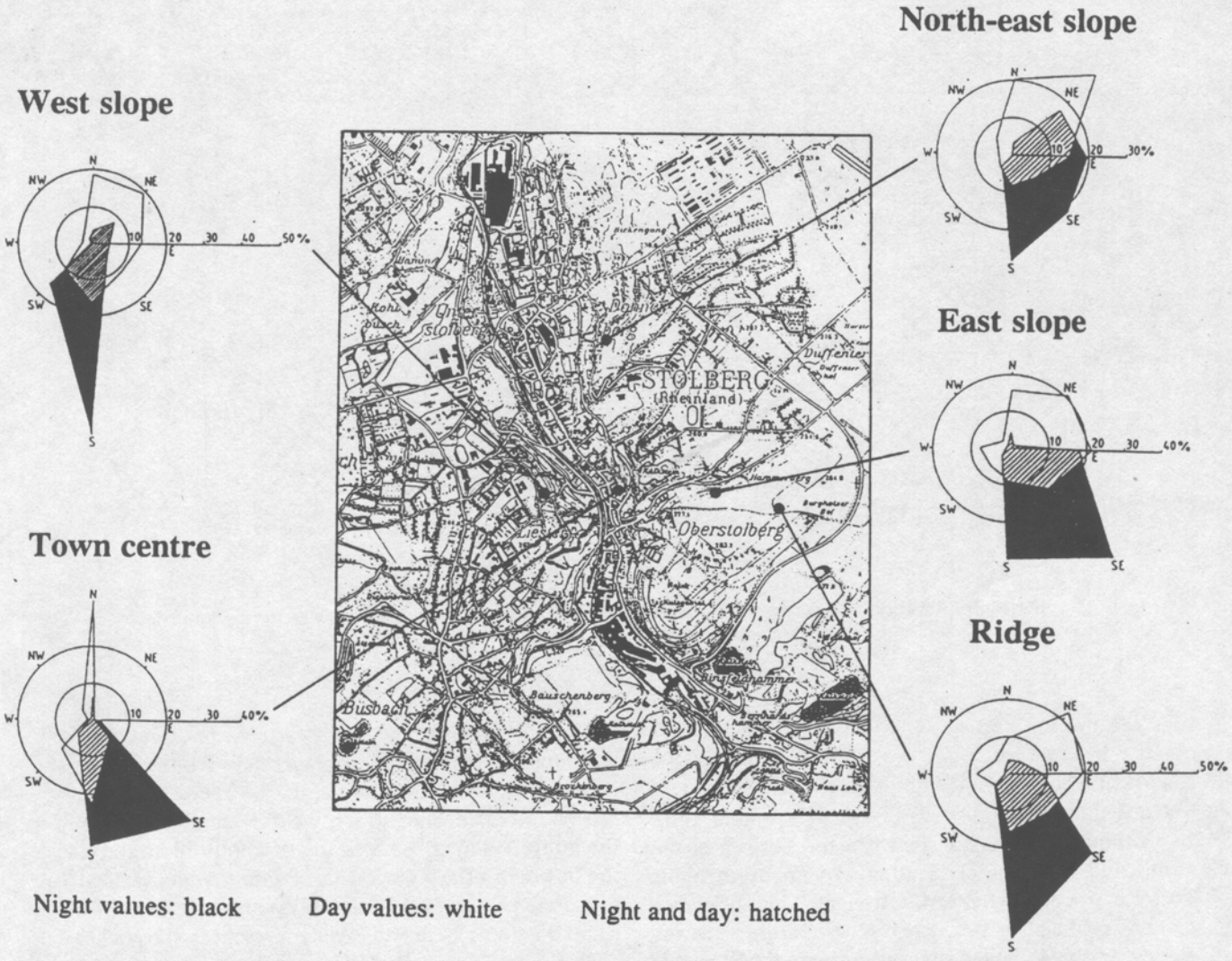

Fig. 7. Distribution of wind directions (%) at selected stations in Stolberg, divided in daytime and nighttime hours based on data obtained from 41 days with cloudless and nearly calm weather conditions in measuring period from June 1990 to April 1991.

Table 9. Number of hours with isothermal or inversion temperature gradients for selected sections of Vichtbach Valley in Stolberg. Measuring period: June 1990–April 1991

Temperature gradient (K for 100 m)	Valley bottom–Upper slope				Valley bottom–Lower slope			
	Station pairs 3 and 4		Station pairs 6 and 4		Station pairs 3 and 2		Station pairs 6 and 2	
	Hours	%	Hours	%	Hours	%	Hours	%
0.0 < 1.0	797	46.9	1268	32.6	258	24.9	276	7.7
0.0 < 2,0	291	17.1	674	17.3	306	29.5	679	19.0
2.0 < 3.0	241	14.2	391	10.1	189	18.2	537	15.0
3.0 < 4.0	135	7.9	271	7.0	88	8.5	367	10.3
4.0 < 5.0	93	5.5	277	7.1	54	5.2	289	8.1
5.0 < 6.0	43	2.5	233	6.0	42	4.0	223	6.2
6.0 < 7.0	41	2.4	181	4.7	29	2.8	201	5.6
7.0 < 8.0	23	1.4	129	3.3	22	2.1	186	5.2
8.0 < 9.0	12	0.7	129	3.3	15	1.4	185	5.2
9.0 < 10.0	4	0.2	105	2.7	6	0.6	112	3.1
≥ 10.0	20	1.2	227	5.8	29	2.8	525	14.7
$\sum$	1,700	100	3,885	100	1,038	100	3,580	100
Sum referred to data basis	25%		56%		15%		52%	

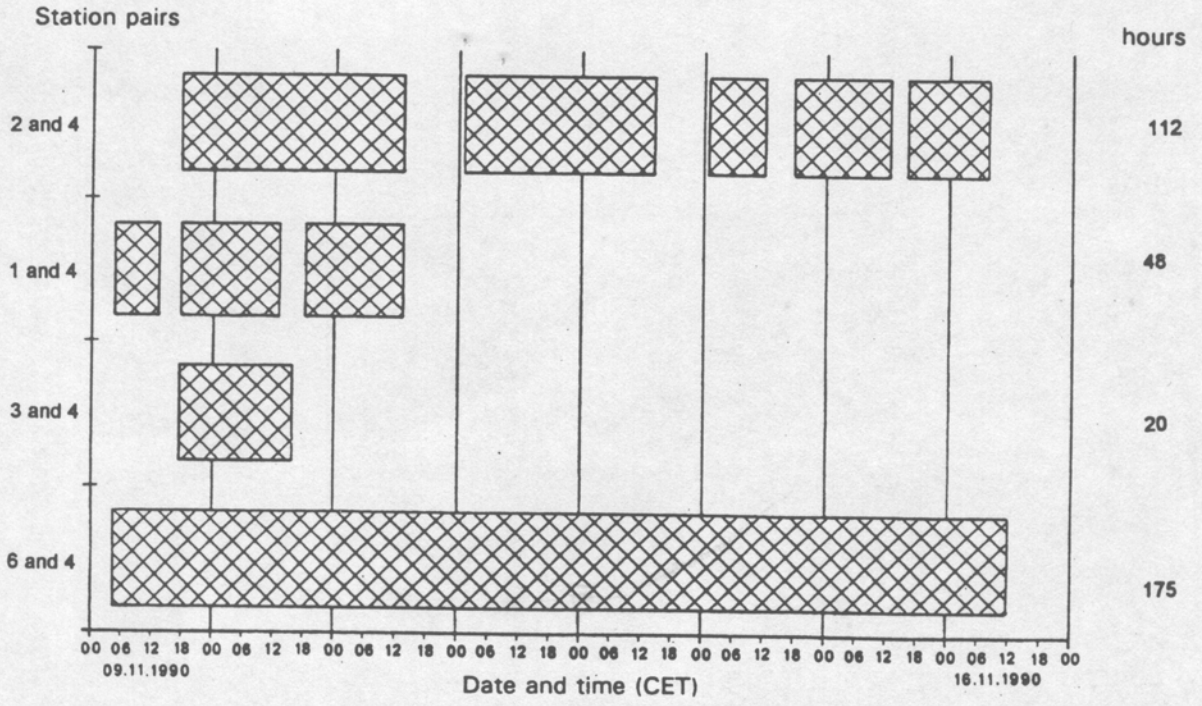

Fig. 8. Comparison of duration of inversion episodes between selected station pairs in Stolberg during an inversion period from 09.11.1990 to 16.11.1990.

tops (Stations 3 and 4). This was encountered frequently in the vertical section from 35 m above the town centre to the rounded hilltops (Stations 2 and 4).

Consequently, Table 9 also verifies the higher number of hours of inversion between the bottom of the valley and upper slope (Station 4) compared to the bottom to ridge distance (Station 5). This difference can be explained by the increased temperatures at the slope (Station 4), which suggests a thermal belt in this region at about 50 to 70 m above the valley bottom. As a consequence of the thermal belt in the northwestern as well as in the south-eastern area, a more or less continuous inversion sublayer between the colder air in the valley and warmer air in the free atmosphere is encountered during inverse weather conditions over the entire valley at an altitude of about 70 m above the bottom of the valley. This certainly limits vertical exchange processes considerably. Consequently, only a small volume of mixed layer is present in the Vichtbach Valley, which often shows unstable layers within the first decametres above the ground in the area of the town centre.

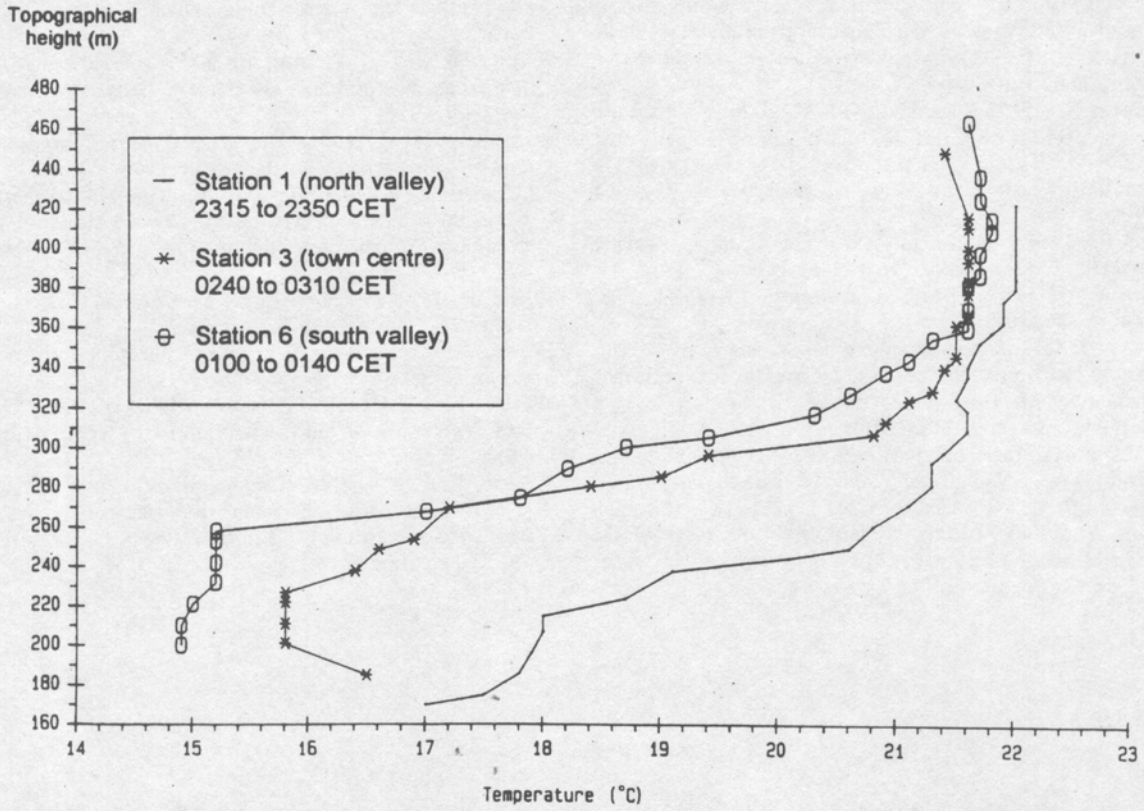

Fig. 9. Vertical profile of air temperature measured by captive balloon ascent (measuring period: 28/29.08.1990).

This phenomenon was confirmed by captive balloon soundings (Fig. 9). A distinct inversion layer at heights between 50 and 70 m above ground, acting as a blocking layer, was observed over the three locations of balloon ascent along the longitudinal profile of the valley, providing the height of the inversion layer defined by the climatological stations. While a distinct ground level inversion exists in the southern Vichtbach Valley, the negative temperature gradient in the first 20 m above the town centre indicates a lifted inversion phenomenon due to the heat island effect.

5. CONCLUSION

Results show that the heat island character of a town located in a valley is influenced during clear and calm weather conditions in different ways by cold air production and dynamics. Determining elements are the dimensions of areas producing cold air, width of the valley, its inclination and roughness of its surfaces. The heavily built up town centre combined with the narrowness of the valley obstruct cold air drainage at night; consequently cold air cannot penetrate into the urban area in the first half of the night. This leads to high excess temperatures (Δt_{u-r}) between the urban and rural areas in the valley during that time. Temperature differences may reach 6 K, corresponding to the relationship between the heat island effect and population described by Oke (1991). It was proved that the degree of this temperature difference was primarily determined by the rate of sealed area.

In contrast to heat islands of large cities, in which excess heating is continued until shortly before sunrise (Landsberg, 1981; Kuttler, 1988), an accelerated reduction of the heat island effect occurs during the night, with an increased production of cold air in the area. Because of the increased movement of cold air in the urban built up area during the second half of the night, higher cooling rates of the air temperature were determined in this region than in the thermal belt. This result is also confirmed for large cities in basins (Dittmann, 1982). An analysis of the mountain and valley wind regime, as well as the examination of vertical temperature distributions, showed that the majority of cold air drains off above the UCL in the second half of the night, while only a small volume flows through the built up area with low velocities near the ground; this suppresses the heat island effect.

REFERENCES

Barlag A.-B. (1993) Planungsrelevante Klimaanalyse einer Industriestadt in Tallage—dargestellt am Beispiel der Stadt Stolberg (Rhld.). *Essener Ökologische Schriften*, Bd. 1, 185 pp. Essen.

Barlag A.-B. and Kuttler W. (1991) The significance of country breezes for urban planning. *Energy and Buildings* **15–16**, Vol. 2, 291–297.

Danzeisen H. (1983) Experimentelle Untersuchung bodennaher Lufttemperatur- und Feuchteverteilungen in Stadtgebieten mit Hilfe eines Meßwagens. *Beiträge Landschaftspflege Rheinland-Pfalz* **9**, 7–34.

Dittmann C. (1982) Regensburg — Stadtklima und Lufthygiene. *Acta Albert. Ratisb.* Bd. **41**, 336 pp. Regensburg.

Garstang M., Tyson P. D. and Emmitt G. D. (1975) The structure of heat islands. *Rev. Geophys. Space Phys.* **13**, 139–165.

Geiger R. (1961) *The Climate Near the Ground.* Harvard University Press, Cambridge, 611 pp.

Goldreich Y. (1984) Urban topoclimatology. *Prog. Phys Geog.* **8**, 336–364.

Gross G. (1983) Influencing an urban heat island by nocturnal cold air drainage; a numerical simulation experiment. *Annalen der Meteorologie* **20**, 59–61.

Horbert M., Schäpel C. and v. Stülpnagel A. (1991) Klimauntersuchungen im Rahmen von Sanierungsmaßnahmen in Goslar-Oker. *Naturschutz und Landschaftsplanung* **1**, 19–27.

Kuttler W. (1988) Spatial and temporal structures of the urban climate — a survey. In *Environmental Meteorology* (edited by Grefen K. and Löbel J.), 305–333. Dordrecht.

Kuttler W. (1993) Planungsorientierte Stadtklimatologie. Aufgaben, Methoden, Fallbeispiele. *Geogr. Rdsch.*, H. 2, Jg. **45**, 95–106.

Landsberg H. E. (1981) *The urban climate.* International Geophysics Series. Vol. **28**, 275 pp. New York.

Nkemdirim L. C. (1980) Cold air drainage and temperature fields in an urban environment: a case study of topographical influence on climate. *Atmospheric Environment* **14**, 375–381.

Oke T. R. (1991) *Boundary Layer Climates*, 2nd Edn, 435 pp. Methuen, London and New York.

Wanner H. and Filliger P. (1989) Orographic influence on urban climate. *Weather Climate* **9**, 22–28.

Wanner H. and Hertig J. A. (1984) Studies of urban climate and air pollution in Switzerland. *J. Appl. Met.* **23**, 1614–1625.

Wiesner K. P. (1986) Programme zur Erfassung von Landschaftsdaten, eine Bodenerosionsgleichung und ein Modell der Kaltluftentstehung. *Heidelb. Geogr. Arb.*, H. **79**, 83 pp., Heidelberg.